Harmonic Distortion Analysis via Perturbation Methods

K. Odame, P. E. Hasler
School of Electrical and Computer Engineering
Georgia Institute of Technology, Atlanta, Georgia 30332–0250
odame@ece.gatech.edu

***Abstract*— The most commonly-used analytical tool for predicting distortion is Volterra series. Analog circuits that yield to Volterra series analysis can also be analyzed with perturbation theory. In fact, perturbation methods can even be used to study certain distortion phenomena that are inscrutable with Volterra series analysis. This paper describes some elementary results that come from applying perturbation methods to simple first-order circuits.**

I. Why not Volterra Series?

Whenever designers want to get an analytical handle on the sources and causes of distortion, the most commonly-used tool is Volterra series analysis. If a problem is tractable using Volterra series, then it can also be solved with perturbation theory, which will yield asymptotically-identical results [1].

There are certain problems for which Volterra series are ill-suited – multiple-time-scale behavior and multiple steady states, for instance [2]– that can be solved with perturbation theory. Despite the power of perturbation theory, it is still a relatively obscure concept in discussions about nonlinearity and distortion in analog circuits. We therefore find it worthwhile to give a basic treatment of regular perturbation – the simplest perturbation method – as applied to distortion analysis of first-order analog circuits. Our treatment will illustrate how well-known tenets of low-distortion design, such as feedback, are readily derived from the perturbation method.

II. Regular Perturbation

Consider the initial value problem

$$\dot{x} = f(t, x, \epsilon); x(t_0) = x_0(\epsilon), \tag{1}$$

where ϵ is a small perturbation parameter such that $\epsilon = 0$ yields an analytically-soluble equation. If f is sufficiently smooth[1], then the problem has a unique solution $x(t, \epsilon)$. As the solution for $\epsilon \neq 0$ may not be analytical, it can be approximated as a power series in ϵ to an accuracy of $\mathrm{O}(\epsilon^{n+1})$. That is, we can write the solution as

$$x(t, \epsilon) = \underbrace{\sum_{i=0}^{n} \left(x_i(t)\epsilon^i\right)}_{\hat{x}(t,\epsilon)} + \mathrm{O}(\epsilon^{n+1}) \tag{2}$$

where $\hat{x}(t, \epsilon)$ is the approximate solution. To conduct regular perturbation, we apply the substitution $x(t, \epsilon) \approx \hat{x}(t, \epsilon)$ to (1).

[1]The specific smoothness requirements of f are discussed in [4]

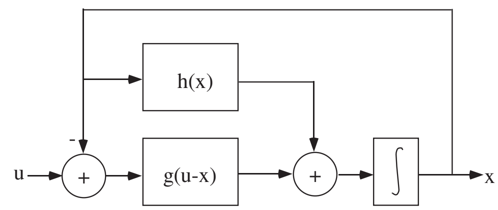

Fig. 1. General block diagram form of a first-order circuit. The primary processing block is $g(\cdot)$, which is a nonlinear function of the input u and of x via feedback. The nonlinearity $h(x)$ models such nonidealities as finite output impedance.

The resulting system is then solved by equating like powers of ϵ. The following sections will illuminate this idea.

III. The Basic First-Order Circuit

Most common first-order analog ciruits (simple amplifiers, buffers, switches, etc.) are of the form depicted in Fig. 1. The governing equation is

$$\dot{x} = g(u - x) + h(x), \tag{3}$$

where u is the a.c. input signal, x is the a.c. output signal and $g(\cdot)$ and $h(\cdot)$ are nonlinear functions. The dependence of the system on the output, other than through feedback to the input, is modeled by $h(x)$. In practice, $h(x)$ is typically some non-ideality such as finite output resistance.

In order to apply perturbation analysis to (3), we begin by assuming that the input signal has a small amplitude. This is expressed as $u = \epsilon v$, where ϵ is a small perturbation parameter and v is a suitably-scaled version of the input signal. Note that with the definition of u, (3) is solvable via separation of variables for the special case $\epsilon = 0$.

With the introduction of the perturbation parameter ϵ, we can approximate the solution to (3) with the power series

$$x(t) \approx \sum_{i=1}^{n} \epsilon^i x_i(t). \tag{4}$$

Note the ϵ^0 term of (4) is set to 0. This corresponds to analyzing a circuit about its d.c. bias point, where the d.c. bias point is shifted to the origin. For ease of notation, define $z = u - x$. The approximation of z is defined similarly to (4), with $z_1 = v - x_1$ and $z_i = -x_i, \forall\ i > 1$.

978-1-4244-2167-1/08/$25.00 ©2008 IEEE

If ϵ is sufficiently small, then the functions $g(z)$ and $h(x)$ can be approximated by their truncated Taylor series as

$$\begin{aligned} g(z) &\approx g_1 z + g_{n-1} z^{n-1} + g_n z^n \\ h(x) &\approx h_1 x + h_{n-1} x^{n-1} + h_n x^n, \end{aligned} \quad (5)$$

Functions g and h are assumed to be dominantly $(n-1)^{\text{th}}$-order nonlinearities, with $g_i = g^{(i)}(0)/i!$ and $h_i = h^{(i)}(0)/i!$. Equation (5) assumes $g(0) = h(0) = 0$, which, again, corresponds to analyzing a circuit about its d.c. bias point.

Substituting (4) and (5) into (3) and collecting powers of ϵ, we get the following set of first-order *linear* equations

$$\begin{aligned} \dot{x}_1 + (g_1 - h_1)x_1 &= g_1 v \\ &\vdots \\ \dot{x}_k + (g_1 - h_1)x_k &= 0 \quad \forall\, k < n-1 \\ &\vdots \\ \dot{x}_{n-1} + (g_1 - h_1)x_{n-1} &= g_{n-1} z_1^{n-1} + h_{n-1} x_1^{n-1} \\ \dot{x}_n + (g_1 - h_1)x_n &= g_n z_1^n - n g_{n-1} z_1^{n-1} x_2 + \\ & \quad h_n x_1^n - n h_{n-1} x_1^{n-1} x_2. \end{aligned} \quad (6)$$

The ϵ^1 equation is the linearized portion of (3) with input v. Taking the Laplace transform of this equation, we write

$$X_1(s) = g_1 H(s) V(s), \quad (7)$$

where $H(s) = 1/(s + g_1 - h_1)$.

The ϵ^k equations ($k < (n-1)$) are filters with 0 input. As such, the steady state solutions of these equations is 0.

IV. Harmonic Distortion Terms

The inputs of the ϵ^{n-1} equation are terms of z_1^{n-1} and x_1^{n-1}. To understand the implications of these terms to harmonic distortion, assume a single-tone input, $v = cos(\omega t)$. This elicits the signals

$$\begin{aligned} x_1 &= g_1 |H(j\omega)| \cos(\omega t + \phi(j\omega)) \\ z_1 &= |1 - g_1 H(j\omega)| \cos(\omega t + \phi_{z1}(jw)) \\ &= |\underbrace{(s - h_1) H(j\omega)}_{H_{z1}(j\omega)}| \cos(\omega t + \phi_{z1}(jw)) \end{aligned} \quad (8)$$

Here we have defined $H_{z1}(s) = (1 - g_1 H(s))$. The phases $\phi(s)$ and $\phi_{z1}(s)$ are the arguments of $H(s)$ and $H_{z1}(s)$, respectively. The signals x_1 and z_1 are single tones of frequency ω as well, since they are merely linearly-filtered versions of v.

Raising z_1 and x_1 each to the $(n-1)^{\text{th}}$ power produces harmonics as follows. If $(n-1)$ is odd(even), then odd(even) harmonics up to the $(n-1)^{\text{th}}$ harmonic are generated. The amplitude of the $m\omega$ frequency term in x_1^{n-1} is

$$\frac{(n-1)!\,g_1}{\frac{n+m-1}{2}!\,\frac{n-m-1}{2}!\,2^{n-2}} |H(j\omega)|, \quad (9)$$

while that of the $m\omega$ frequency term in z_1^{n-1} is

$$\frac{(n-1)!}{\frac{n+m-1}{2}!\,\frac{n-m-1}{2}!\,2^{n-2}} |H_{z1}(j\omega)|. \quad (10)$$

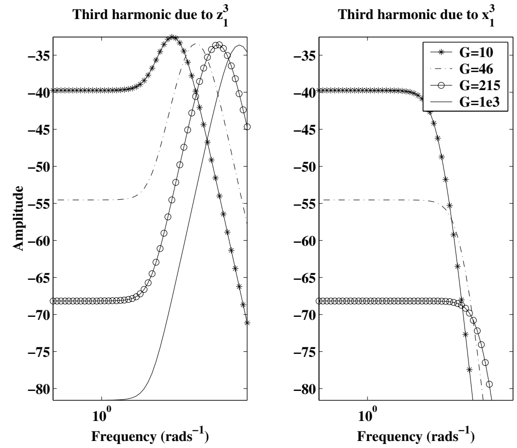

Fig. 2. Magnitude-frequency plots of the third harmonic. The 'gain', G of the $g(z)$ function is varied from 10 to 1000. This causes the band-pass shape of the z_1^3-contributed harmonic to shift to the right, while that contributed by x_1^3 falls in magnitude.

After filtering in the ϵ^{n-1} equation, the amplitudes of these terms will be, respectively,

$$\frac{(n-1)!\,h_{n-1} g_1}{\frac{n+m-1}{2}!\,\frac{n-m-1}{2}!\,2^{n-2}} |H(j\omega)||H(jm\omega)|, \quad (11)$$

and

$$\frac{(n-1)!\,g_{n-1}}{\frac{n+m-1}{2}!\,\frac{n-m-1}{2}!\,2^{n-2}} |H_{z1}(j\omega)||H(jm\omega)|. \quad (12)$$

Analogous to that of the ϵ^{n-1} equation, the input to the ϵ^n equation has terms in z_1^n and x_1^n. In general, the x_2 terms are identically zero, except for the special case $n = 3$.

V. Feedback and Distortion

We now make some observations about the harmonic distortion results that were discussed in the previous section.

In the ϵ^{n-1} equation, the amplitude of the m^{th} harmonic that the z_1^{n-1} term contributes is given by (12). We plot this amplitude expression, along with that of (11), as a function of frequency in Fig. 2 for the third-order harmonic generated by a dominantly-third order nonlinearity. That is, $n = 4$ and $m = 3$. Also, we chose $h_1 = 1$, $h_3 = 1/3$, $g_1 = G$, $g_3 = G/3$, where G was varied from 10 to 1000.

Notice from the figure that if $g_1 \gg h_1$, then, for a given frequency, the amplitude of the z_1^{n-1}-contributed harmonic is greatly reduced. In fact, if we ensure $g_i \gg h_i\ \forall\ i$, then the harmonic contribution of the x_1^{n-1} terms is negligible. This would mean that the distortion is effectively due only to z_1, whose associated harmonics are band-pass filtered. This in turn means that the distortion can be kept small if the circuit is operated well below the corner frequency.

These two notions – that frequency and feedback gain can be sacrificed for higher linearity – conform with the traditional rules-of-thumb for low-distortion design.

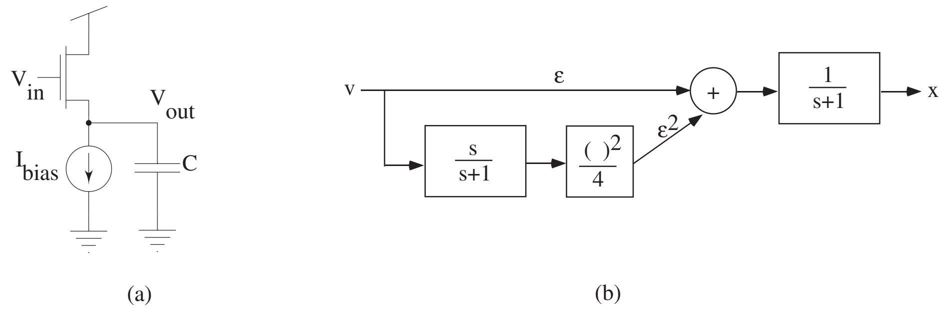

Fig. 3. Source follower amplifier. (a) Circuit schematic. (b) Block diagram representation of source follower output. The fundamental harmonic is a low-pass filtered version of the input. The second order terms are generated by high-pass filtering the input, squaring and then low pass filtering. The total output is a power series of ϵ terms.

VI. Illustrative Examples

A. *Source Follower Amplifier*

According to KCL, the circuit equation of the source follower amplifier in Fig. 3 (a) is

$$C\frac{dV_{\rm out}(t)}{dt} = F(V_{\rm in}, V_{\rm out}) - I_{\rm bias}, \tag{13}$$

where the function F is defined as

$$F(V_{\rm in}, V_{\rm out}) = \frac{K}{2}\left(\kappa V_{\rm in}(t) - V_{\rm out}(t) - V_{\rm th}\right)^2, \tag{14}$$

if M_1 is in above-threshold saturation, and

$$F(V_{\rm in}, V_{\rm out}) = I_{\rm o}e^{(\kappa V_{\rm in}(t) - V_{\rm out}(t))/U_{\rm T}}, \tag{15}$$

if it is in subthreshold saturation. The parameter K depends on transistor dimensions and doping and $V_{\rm th}$ is the threshold voltage. Also, κ, $I_{\rm o}$ and $U_{\rm T}$ have their usual meanings from the EKV MOSFET model [3].

Note that $I_{\rm bias} = F(V_{\rm G}, V_{\rm S})$, where $V_{\rm G}$ and $V_{\rm S}$ are the d.c. bias-points of the gate and source of M_1, respectively. Let us define a *characteristic voltage*, $V_{\rm c}$, as

$$V_{\rm c} = \begin{cases} (\kappa V_{\rm G} - V_{\rm S} - V_{\rm th})/2, & \text{above threshold} \\ U_{\rm T}, & \text{subthreshold.} \end{cases} \tag{16}$$

Now, (13) can be non-dimensionalized [4] by making the substitutions

$$\tau = I_{\rm bias}/(CV_{\rm c}) \cdot t; \quad u = \kappa\nu_{\rm in}/V_{\rm c}; \quad x = \nu_{\rm out}/V_{\rm c}, \tag{17}$$

where $\nu_{\rm in}$ and $\nu_{\rm out}$ are the a.c. portions of $V_{\rm in}$ and $V_{\rm out}$. This gives the state-space equation of the source follower as

$$\frac{dx}{d\tau} = u - x + (u-x)^2/4, \tag{18}$$

for above threshold, and

$$\frac{dx}{d\tau} = u - x + (u-x)^2/2, \tag{19}$$

for the truncated Taylor expansion in subthreshold. The point is that, regardless of region of operation of M_1, the nonlinear equation that describes the source follower has the same functional form. Relating the source follower equations to (3), we have $g(z) \sim z + z^2$ and $h(x) = 0$. As such, we expect the harmonic distortion terms to have a band-pass-like dependence on frequency. To show this, we will apply regular perturbation to (18).

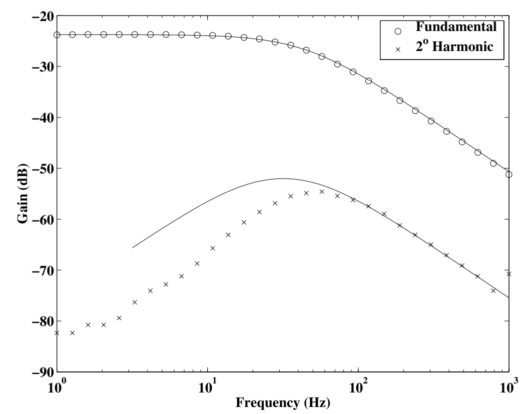

Fig. 4. Magnitude-frequency response of source follower. Analytical prediction is in bold, and experimental data is plotted as ‘x’s and ‘o’s. The fundamental harmonic is a low-pass filtered version of the input. The second harmonic has a bandpass shape, as predicted by perturbation analysis.

First, define $u = \epsilon v$, where the small parameter ϵ is a scaled version of the input amplitude. That is, $\epsilon = A_{\rm in}/V_{\rm c}$. Also, taking $x = \epsilon x_1 + \epsilon^2 x_2$ and $z = u - x$ and equating like powers of ϵ up to ϵ^2, we have

$$\epsilon^1: \quad \dot{x}_1 = v - x_1 \tag{20}$$

$$\epsilon^2: \quad \dot{x}_2 = z_1^2/4 - x_2 \tag{21}$$

Assume a pure-tone input, $v = \cos(\omega t)$. Equation (20) is the linear portion of the amplifier. Equation (21) is a linear filter with input $z_1^2/4$. The squaring produces a second-harmonic term as well as a d.c. offset. In addition, since $z_1 = v - x_1$, the second-harmonic generated by the squaring is high-pass filtered. The overall effect is that x_2 is a band-pass filtered version of a second harmonic of v. Figure 4 is a plot of experimental data that corroborates our analysis.

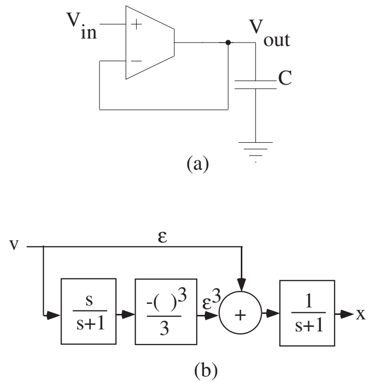

Fig. 5. Unity gain buffer. (a) Circuit schematic. (b) Block diagram representation of output. The fundamental harmonic is a low-pass filtered version of the input. The third-order terms are generated by high-pass filtering the input, cubing and then low pass filtering. The total output is a power series of ϵ terms.

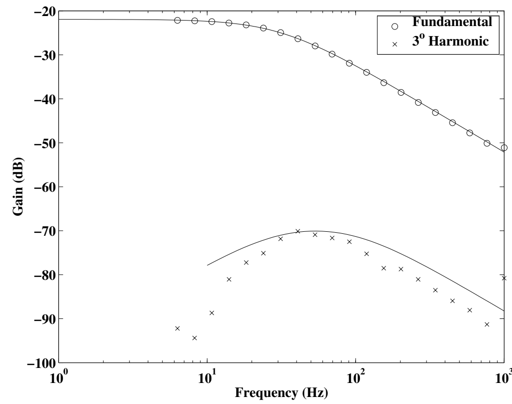

Fig. 6. Magnitude-frequency response of unity-gain buffer . Analytical prediction is in bold, and experimental data is plotted as ‘x’s and ‘o’s. The fundamental harmonic is a low-pass filtered version of the input. The third harmonic has a bandpass shape, as predicted by perturbation analysis.

B. Unity Gain Buffer

Consider the unity-gain buffer depicted in Fig. 5 (a). It is formed by placing an operational transconductance amplifier (OTA) in negative feedback. If we operate the OTA above threshold, the describing equation is

$$C\frac{dV_{\rm out}}{dt} = \sqrt{\kappa\beta I_{\rm bias}}V_{\rm in}\sqrt{1-\frac{\kappa\beta V_{\rm in}^2}{4I_{\rm bias}}}, \tag{22}$$

while it is

$$C\frac{dV_{\rm out}}{dt} = I_{\rm bias}\tanh\left(\frac{\kappa V_{\rm in}}{2U_{\rm T}}\right), \tag{23}$$

for subthreshold operation. Notice that we have ignored the output conductance term, which is considered very small for OTAs.

We can define a characteristic voltage, $V_{\rm c}$, as

$$V_{\rm c} = \begin{cases} \frac{2U_{\rm T}}{\kappa}, & \text{subthreshold} \\ \sqrt{\frac{I_{\rm bias}}{\kappa\beta}}, & \text{above threshold.} \end{cases} \tag{24}$$

Then, with the following definitions

$$\tau = I_{\rm bias}/(CV_{\rm c})\cdot t; \quad u = \nu_{\rm in}/V_{\rm c}; \quad x = \nu_{\rm out}/V_{\rm c}, \tag{25}$$

the nondimensional form of the unity-gain buffer's describing equations (taken to the first few Taylor series terms) is

$$\frac{dx}{d\tau} = \begin{cases} (u-x)-(u-x)^3/4, & \text{above threshold} \\ (u-x)-(u-x)^3/3, & \text{subthreshold.} \end{cases} \tag{26}$$

Again, the functional form of the equations is identical, regardless of region of operation.

To calculate distortion terms, assume $u = \epsilon v$ is a pure-tone signal and proceed as usual. For subthreshold, the separated equations of ϵ are

$$\epsilon^1: \quad \dot{x}_1 = v - x_1 \tag{27}$$
$$\epsilon^2: \quad \dot{x}_2 = 0 - x_2 \tag{28}$$
$$\epsilon^3: \quad \dot{x}_3 = z_1^3/3 - x_3. \tag{29}$$

Equation (27) is the linear portion of the amplifier. Equation (28) is a linear filter with 0 input; it contributes no harmonics at steady state. Equation (29) is a linear filter with input $z_1^3/3$. The cubing produces a third-harmonic term as well as a fundamental-frequency term (this fundamental-frequency term will cause gain compression, which is not discussed in this paper). Since $z_1 = v - x_1$, the overall effect is that x_3 is a band-pass filtered version of a third harmonic of v, as shown in Fig. 6.

C. Note on above-threshold versus subthreshold operation

The harmonic behavior of a circuit is similar for above- and subthreshold operation. In absolute numbers, however, above threshold operation yields less distortion. This is because the parameter $\epsilon = A_{\rm in}/V_{\rm c}$ is much smaller for above threshold than for subthreshold. Since the harmonics are multiplied by ϵ^i, the smaller ϵ seen in above threshold operation translates to lower distortion.

VII. Conclusion

In this paper, we have examined the problem of harmonic distortion via perturbation analysis. Our approach yields information about the various processing flows that are responsible for each harmonic term. We have provided various examples of the technique and have compared our analytical predictions to experimentally-measured data.

References

[1] A. Buonomo and A. Lo Schiavo, “Perturbation analysis of nonlinear distortion in analog integrated circuits,” *TCASI: Fundamental Theory and Applications*, vol. 52, no. 8, pp. 1620–1631, 2005.

[2] R. Rand, *Lecture Notes on Nonlinear Vibrations*, The Internet-First University Press, Ithaca, NY, 2003.

[3] C. C. Enz, F. Krummenacher, and E. A. Vittoz, “An analytical mos transistor model in all regions of operation and dedicated to low-voltage and low-current applications,” *Analog Integrated Circuits and Signal Processing*, vol. 8, no. 1, pp. 83–114, 1995.

[4] S. H. Strogatz, *Nonlinear Dynamics and Chaos*, Westview, Cambridge, MA, 1994.